Density functional theory investigations of radical scavenging activity of 30-Methyl-quercetin

4 AUTHORS:

Abdullah Al-sehemi
King Khalid University
172 PUBLICATIONS **835** CITATIONS

SEE PROFILE

Ahmad Irfan
Changchun Normal University
85 PUBLICATIONS **652** CITATIONS

SEE PROFILE

Salha Mana Aljubiri
King Khalid University
2 PUBLICATIONS **1** CITATION

SEE PROFILE

Kamel Shaker
King Khalid University
53 PUBLICATIONS **297** CITATIONS

SEE PROFILE

ORIGINAL ARTICLE

Density functional theory investigations of radical scavenging activity of 3′-Methyl-quercetin

Abdullah G. Al-Sehemi [a,b,*], **Ahmad Irfan** [a,*], **Salha Mana Aljubiri** [a], **Kamel Hussein Shaker** [a]

[a] *Department of Chemistry, Faculty of Science, King Khalid University, Abha 61413, P.O. Box 9004, Saudi Arabia*
[b] *Unit of Science and Technology, Faculty of Science, King Khalid University, Abha 61413, P.O. Box 9004, Saudi Arabia*

Abstract The possible eight rotamers of 3′-Methyl-quercetin have been optimized by using density functional theory (DFT) at B3LYP/6-31G* level of theory. The molecular structure and molecular properties of the most stable rotamers have been investigated at the same level of theory. We have computed the descriptors; electronegativity (χ), hardness (η), electrophilicity (ω), softness (S) and electrophilicity index (ωi) by DFT approach. We have shed light on the structure–property relationship. The absorption spectrum has been computed by time dependent density functional theory (TD-DFT) at TD-B3LYP/6-31G* level of theory. Radical scavenging activity has been explained on the basis of bond dissociation enthalpy (BDE) and the adiabatic ionization potential (IP). Two mechanisms have been explained for the radical scavenging processes, i.e., hydrogen atom transfer and one-electron transfer.

1. Introduction

The genus *Bassia* is a member of the family Chenopodiaceae. Genus *Bassia* includes many of the species that are distributed in the deserts. The species of genus *Bassia* are annual or perennial subshrubs. The literature showed that only a few species of *Bassia* have been investigated and were found to contain triterpenoidal saponins identified as basic acid glycosides (Rizk, 1986; Kamel et al., 2001), and the presence of flavonoids, phenolic acids, fatty acids, hydrocarbons, sterols, volatile oils (El-Sayed et al., 1998) and saponins (Kamel et al., 2001). *Bassia muricata* is used in folk medicine to treat renal and rheumatic diseases (Al-Yahya et al., 1990). The chloroform and ethanolic extracts of the plant produced pilo-erection, significant hypotension, a remarkable decrease in WBC (White Blood Cell or Leukocyte) counts, and a significant increase in prothrombin time besides their significant contractions of isolated guinea pig ileum. Meanwhile, the ether and benzene extracts showed antimicrobial activities (Al-Yahya et al., 1990).

On the other hand, the whole plant of *Bassia muricata* possesses different degrees of antiinflammatory, analgesic and antipyretic effects as well as antispasmodic property (El-Khatib and Khaleel, 1995) and the chloroform extract was active

* Corresponding authors. Tel.: +966 72418632; fax: +966 72418426.
E-mail addresses: agmasq@gmail.com (A.G. Al-Sehemi), irfaahmad@gmail.com (A. Irfan).

against *Spodoptera littoralis* and *Agrotis ipsilon*. Fungicidal activity was also detected (El-Sayed et al., 1998). Oxidative stress induced by reactive oxygen species and reactive nitrogen species such as the superoxide anion radical, hydroxyl radical, lipid peroxyl radical, or peroxynitrite, can cause damage to cellular proteins, membrane lipids and nucleic acids, where this process has been implicated in the pathogenesis of various diseases, including coronary heart disease and some forms of cancer (Pietta, 2000). Flavonoids are the most important class of polyphenolic compounds, which in addition to their important biological roles in plant pigmentation, nitrogen fixation, and chemical defense possess anti-cancer, anti-inflammatory, antibacterial, antiviral, and antiallergic properties that are a consequence of their antioxidant properties (Aron and Kennedy, 2008; Halliwell, 2007; Manach et al., 2005; Rosane et al., 2006).

Polyphenol compounds such as quercetin, (Huang et al., 2010) protocatechuic acid, caffeic acid and a variety of flavonoids are present in fruits and vegetables and are an integral part of the human diet. It is already known that dietary polyphenols show potent antiradical ability. The radical scavenging abilities of these compounds depend greatly on the number and arrangement of phenolic hydroxyl groups. Recently, theoretical methods especially density functional theory (DFT) method, have been successfully used to evaluate chemical properties, such as bond dissociation enthalpy (BDE) and the adiabatic ionization potential (IP) of polyphenol compounds and to elucidate the structure–activity relationship for phenolic antioxidants (Antonczak, 2008). Furthermore, the study of the electronic and molecular properties is of great importance that helps to understand the mechanism of the antioxidant activity of these compounds.

The antioxidant activity of the phenolic constituents is related to their structures. To stabilize the radicals intramolecular hydrogen bonds play a key role (Leopoldini et al., 2004a). The plant *Bassia muricata* is common in Aseer region which is nearly unexplored. So, it is desired to investigate the chemical constituents of the plant as well as its biological activities. In the present study the compound 3′-Methyl-quercetin (SB4) was isolated and identified from *n*-butanol of the alcoholic extract of *Bassia muricata* grown in the Aseer region of KSA. The SB4 contains intramolecular hydrogen bonds between hydroxyl-H and keto-O groups; and hydroxyl-H and methoxy-O, see Fig. 1. However, to the best of our knowledge, no calculation about the antioxidant activity has been reported so far. In this work, the structural, electronic and molecular properties were investigated at the density functional theory level. Our aim is to shed light on the radical scavenging activity and reveal their scavenging capacity through calculation of proper molecular descriptors. Bond dissociation enthalpy (BDE) and ionization potential (IP) values have been used as indicators of the ease by which these molecules can deactivate free radicals. Moreover, by using time dependent density functional theory absorption spectra has been computed.

2. Experimental

2.1. Plant material

The aerial parts of *Bassia muricata* were collected from Abha, Aseer region, Saudi Arabia, in April 2011. The plant was identified by Dr. Mahmoud Fawzy, Biology department, College of Science, King Khalid University. A plant sample had been kept in the Botany department, College of Science, King Khalid University.

2.2. General material

^{1}H NMR (500.13 MHz), ^{13}C NMR (125.75 MHz) and 2D NMR spectra were measured on a Bruker DRX 500 spectrometer (Bruker Biospin, Rheinstetten, Germany). Column chromatography (CC): Polyamide 6 for CC (particle size 50–160 μm – Fluka, Germany), and Sephadex LH-20 (Sigma–Aldrich). Thin-layer chromatography (TLC) was performed on silica gel 60 F254 plates (Merck) and visualized under UV light (at 254 and 366 nm) before and after exposure to 5% alcoholic sulfuric acid solution.

2.3. Extraction and isolation

The air dried plant (1.5 kg) was exhaustively extracted with 85% methanol (30.0 l). The methanol extract was concentrated under reduced pressure at the temperature of 50 °C. The methanol extract (77.08 g) was partitioned using petroleum ether, ethyl acetate and *n*-butanol/water. Each solvent was evaporated till dryness. Thin layer chromatography (TLC) showed the presence of different compounds in each fraction. The *n*-butanol fraction exhibited some interesting compounds, therefore the *n*-butanol fraction (8.37 gm) was subjected to column chromatography on polyamide material and eluted with water, water/methanol (8.5:1.5), (7:3), (5:5), (2:8), (0:10) and the eluted fraction was monitored with TLC. The crude compound was eluted with water/methanol (8.5:1.5) and purified on Sephadex LH-20 to afford pure compound.

2.4. ^{1}H NMR and ^{13}C NMR of Compound

The compound has a yellow color on TLC with solvent system CHCl$_3$/MeOH (8:2). ^{1}H NMR of compound showed two signals at δ 6.21, 6.44 for H-6 and H-8 (d, J = 2 Hz) and three signals at δ 6.95 (d, J = 8.5 Hz), 7.75 (dd), 7.89 (d, J = 2 Hz) for H-5′, H-6′ and H-2′. ^{13}C NMR (Fig. S1) showed the presence of a methoxy group at δ 56.5 (Table S1).

3. Computational detail

Generally two main mechanisms are reported for the radical scavenging processes of chain-breaking antioxidant (ArOH)
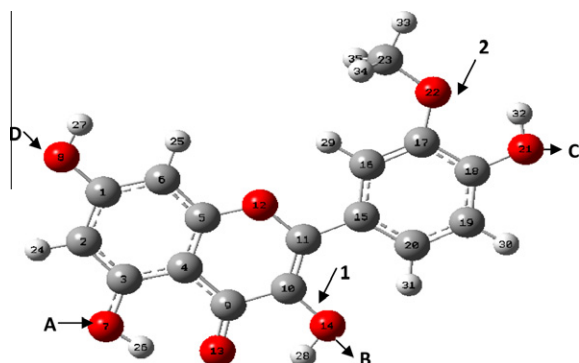

Figure 1   The optimized structure of SB4 with labeling scheme.

(Wright et al., 2001; Leopoldini et al., 2004b; Belcastro et al., 2006): H-atom transfer (Eq. (1)) and one-electron transfer (Eq. (2)):

$$R^{\cdot} + ArOH \rightarrow RH + ArO^{\cdot} \qquad (1)$$

$$R^{\cdot} + ArOH \rightarrow R^{-} + ArOH^{+} \qquad (2)$$

Both mechanisms are important for the scavenging activity of reactive species by an ArOH in chemical or biological system and may occur in parallel. In the H-atom transfer, a free radical $R^{\cdot}$ removes a hydrogen atom from the antioxidant ArOH. The efficiency of the antioxidant ArOH depends on the stability of the radical ArO^{-}, which in turn is determined by the number of hydrogen bonds, conjugation, and resonance effects. The reactivity of an ArOH can be estimated by calculating the O–H bond dissociation enthalpy (BDE), where the lower the BDE value the higher the expected activity. The antioxidants give an electron to the free radical in the one-electron transfer mechanism. Here, the radical cation arising from the electron transfer must be stable. In this case, scavenging activity can be evaluated by the adiabatic ionization potential (IP). Molecules with the low IP and BDE values are expected to have high activity. Thus, in the present study BDE and IP values were used as molecular descriptors in an effort to explain the radical scavenging activity of compounds. All calculations were performed by GAUSSIAN 09 code (Frisch et al., 2009). The ground state geometries have been optimized at the B3LYP/6-31G* level of theory (Irfan and Al-sehemi, 2011; Al-Sehemi et al., 2012, submitted for publication). Harmonic vibrational frequency calculations were performed at the B3LYP/6-31G* level of theory for both parent (ArOH) molecules and radicals (ArO^{-} and $ArOH^{+\cdot}$), to characterize all their conformations as minima or saddle points and to evaluate the zero-point energy (ZPE) corrections, which we have included in all the relative energies, BDE, and IP. The BDE values in gas phase at 298 K were calculated according to the formula BDE = $H_{rad} + H_{hyd} - H_{p}$, where H_{rad} is the enthalpy of the radical generated by H-abstraction, H_{hyd} is the enthalpy of the H-atom, and H_{p} is the enthalpy of the parent molecule. The adiabatic IP values were determined according to the equation IP = $E_{cr} - E_{p}$, where p and cr indicate the parent molecule and the corresponding cation radical generated after electron transfer. The time dependent density functional theory (TD-DFT) has been applied to compute the absorption spectra at the B3LYP/6-31G* level of theory which has been proved to be an accurate and reliable method (Walsh et al., 2006; Cleland et al., 2009). The DOS and UV–Visible Spectrum of these systems were convoluted using GaussSum 2.1 software (O' Boyle et al., 2008). The DFT-based reactivity descriptors were obtained from Eqs. (3)–(7) which play an important role in many areas of research (Kohn et al., 1996; Parr and Pearson, 1983; Chattaraj et al., 1991).

Mulliken electronegativity (χ) was calculated from the following equation:

$$\chi = (E_{HOMO} + E_{LUMO})/2 \qquad (3)$$

Hardness (η) was calculated from the following equation:

$$\eta = (E_{HOMO} + E_{LUMO})/2 \qquad (4)$$

Electrophilicity (ω) was calculated from the following equation:

$$\omega = ((E_{HOMO} + E_{LUMO})/2)^{2}/2\eta \qquad (5)$$

Softness (S) was calculated from the following equation:

$$S = 1/2\eta \qquad (6)$$

Electrophilicity index (ωi) was calculated from the following equation:

$$\omega i = \mu^{2}/2\eta \qquad (7)$$

4. Results and discussions

4.1. Rotamers

In SB4, there are totally four hydroxyl (a–d) and one methoxy (at position 2) group. The hydroxyl groups (a and b) can form hydrogen bond with keto oxygen while hydroxyl group of c can form hydrogen bond with methoxy oxygen. Thus there would be maximum three H-bonding possibilities. According to the H-bonding, we have observed eight rotamers, see Fig. 2. In SB4a, there is one H-bond between hydroxyl-hydrogen (position a) and keto oxygen. In SB4ab, there are two H-bonds between hydroxyl-hydrogens of positions (a and b) and keto oxygen. Three H-bonds exist in SB4abc, two H-bonds between hydroxyl-hydrogens of positions (a and b) and keto oxygen and third between hydroxyl-hydrogen of position c and methoxy-oxygen. Similarly, SB4ac and SB4bc have two hydrogen bonds while SB4b and SB4c have one H-bond. The SB4abc is the most stable rotamer having three H-bonding. Thus we have considered SB4abc rotamer for further investigations, i.e., electronic properties, optical properties, and radical scavenging activities.

4.2. Geometries

The geometrical parameters have been tabulated in Table 1. To explain the radical scavenging activity hydrogen bond plays a vital role. The cutoff values have been suggested as H—A distances < 3.0 Å and D–H—A angles $> 110°$ for D–H—A hydrogen bond (Steiner and Desiraju 1998; Steiner 2002). The interaction between hydroxyl-hydrogens and oxygen of keto while hydroxyl-hydrogen and methoxy-oxygen has been considered for the hydrogen bond. From the data presented in Table 1, it can be seen that H—A is less than 3.0 Å and D–H—A angles are more than 110°.

4.3. Molecular properties

Fig. 3 illustrates the distribution pattern of the highest occupied molecular orbitals (HOMO) and lowest unoccupied molecular orbitals (LUMO). The HOMO is delocalized on entire molecules and the lone pair of electron on the oxygen atoms. The LUMO is of antibonding character with π^{*} distributed on whole of the systems.

The orbital energy level analysis at the B3LYP/6-31G* level showed HOMO energy (E_{HOMO}), LUMO energy (E_{LUMO}) and HOMO–LUMO energy gap (E_{gap}) that has been used as an indicator of kinetic stability of the molecule. E_{HOMO} of SB4 is -5.43 eV and E_{LUMO} is -1.82 eV. The OCH$_3$ and OH groups at positions 2 and 1, respectively lead to higher E_{HOMO}, lower E_{LUMO}, and decrease the E_{gap} compared to luteolin
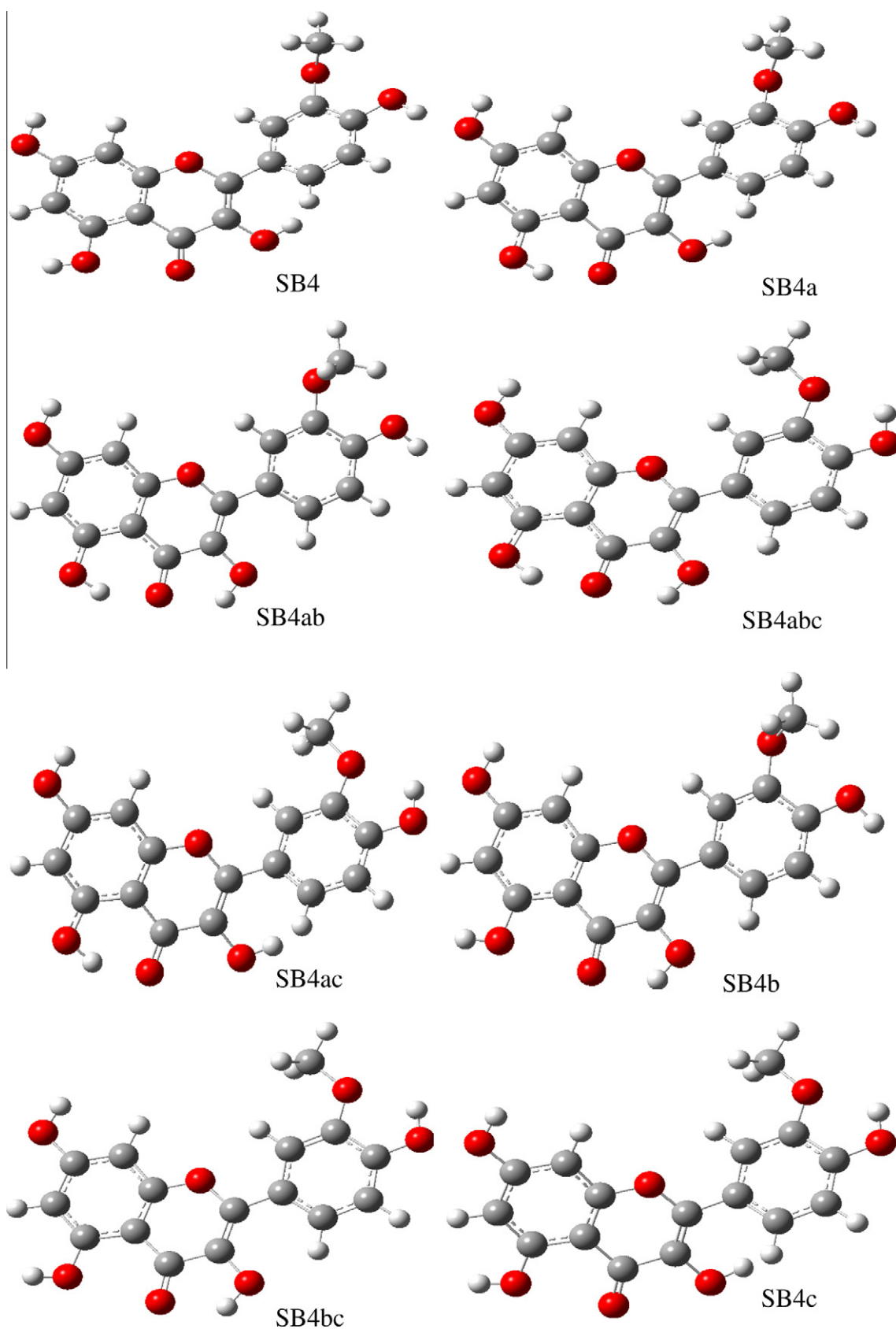
Figure 2   The possible optimized rotamers of SB4 investigated in the present study at B3LYP/6-31G* level of theory.

Table 1 Distances of R_{O-H} and $R_{O\cdots H}$ (Å) and H-bond angles of $\theta_{O-H\cdots O}$ (degree) at B3LYP/6-31G* level of theory.

Parameters	SB4	Parameters	SB4	Parameters	SB4
C3–O7	1.341	C10–O14	1.356	C18–O21	1.357
O7–H26	0.993	O14–H28	0.985	O21–H32	0.974
C9–O13	1.261	C17–O22	1.375	O13…H26	1.762
O13…H28	1.975	O22…H32	2.076	–	–
O7–H26…O13	148.42	O14–H28…O13	120.42	O21–H32…O22	115.20
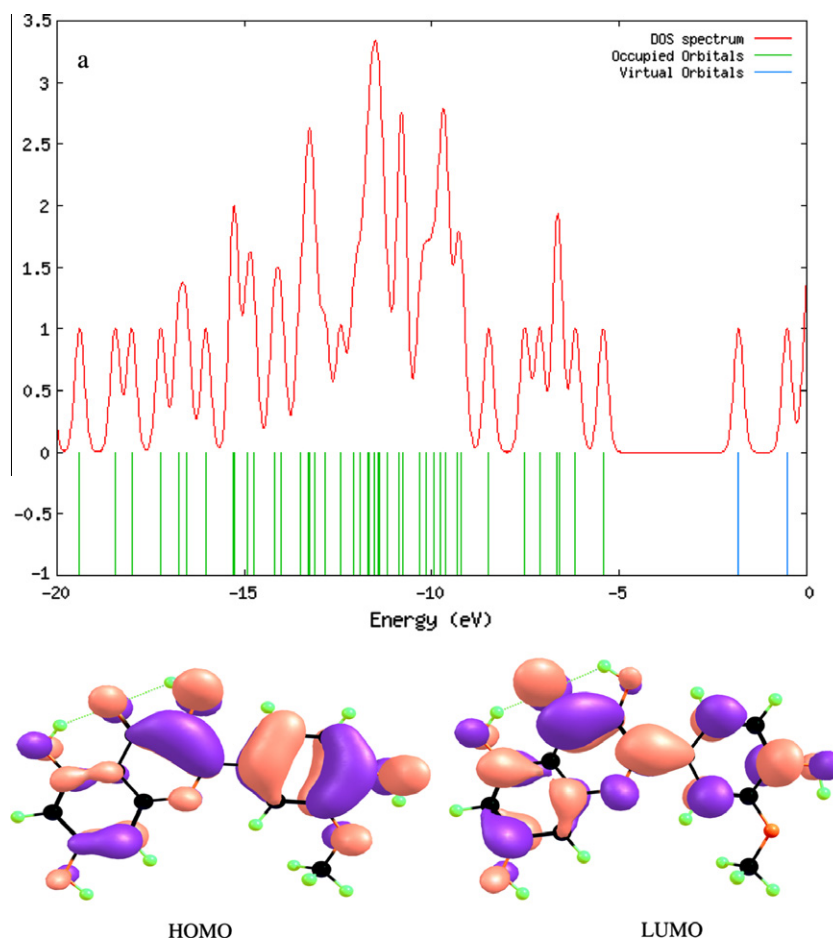
Figure 3 The density of state (top) and distribution pattern of HOMO and LUMO (bottom; color indicates the electron density) at B3LYP/6-31G* level of theory.

(Al-Sehemi et al., 2012, submitted for publication). We have also observed that HOMO and LUMO have almost equal charge density; similarly the first highest occupied molecular orbital (HOMO-1) charge density is similar to HOMO. The second highest occupied molecular orbital (HOMO-2) has a higher charge density than HOMO and HOMO-1, see Fig. 3a. Free radical-scavenging activity of various phenolic antioxidants is also strictly related to the distribution of the HOMO orbital. The molecules with a lower energy HOMO orbital have weaker electron donating ability and revealed that SB4 has higher electron donor ability than luteolin. Besides, the electronic density distribution in these orbitals permits prediction of the most probable sites in the molecules investigated which can be easily attacked by free radicals and other reactive agents. More active redox sites of these molecules are characterized by high density of the HOMO orbital. The contribution to the HOMO from OH groups at b and c positions is greater than that from OH groups at a and d positions. This reveals that b-OH and c-OH are more suitable for the formation of stable radical forms than a-OH and d-OH. Thus, the OH groups at b and c positions can be easily attacked by the free radicals and other reactive agents in the real biological systems which can be verified from Section 4.4.

The chemical hardness is a measure of resistance to charge transfer while the electronegativity is a measure of the tendency to attract electrons by an atom in a chemical bond which is also defined as the negative of the chemical potential in DFT. The electrophilicity index ω represents the stabilization energy of the system and determines the affinity for the electrons and measures. The molecular properties have been

computed for each variable presented in Table 2 revealing that SB4 is capable of giving an electron rather than capturing which in turn is an indication of its antioxidant ability.

4.4. Absorption spectra

The absorption spectrum of SB4 has been presented in Fig. 4. The two absorption peaks are prominent, i.e., at 371 nm which is absorption maxima and the second peak has been observed at 244 nm which are in good agreement with the experimental evidences (see Supporting informations). The maximum absorption spectrum of SB4 is 26 nm red shifted compared to luteolin (Al-Sehemi et al., 2012, submitted for publication). We have computed the absorption wavelengths at the TD-B3LYP/6-31G* level of theory. We have observed peaks at 371 and 244 nm, see Fig. 4. The experimental peaks have been observed approximately at 365 and 260 nm, see Supporting information. There is a complex formed between AlCl$_3$ and the compound (the hydroxyl group at 5-position and carbonyl group at 4-position). This caused a bathochromic shift to 420 nm in comparison to the methanol peak at 365. The complex is stable and cannot be cleaved by the addition of dilute HCl. Electronic transitions up to nine states have been investigated. The S0–S1 state remains dominated with maximum absorption which is caused by HOMO–>LUMO with 94% contribution. The second state caused by HOMO-1–>LUMO with the same contribution like first state. The third state has 77% contribution from HOMO-2–>LUMO. The fourth and fifth states are caused by HOMO-3–>LUMO and HOMO-5–>LUMO, respectively. All of the transitions in sixth, eighth and ninth states have less than 50% contribution from occupied to unoccupied orbitals. The seventh state is derived from HOMO-4–>LUMO with 58% contribution (see Supporting information).

4.5. Hydrogen atom transfer mechanism

By hydrogen abstraction, we have acquired four radicals for the most stable rotamer of SB4, i.e., SB4abc. In SB4a, SB4b, SB4c and SB4d radicals the hydrogen atoms have been abstracted from positions a, b, c and d, respectively. Single radical cation for each parent molecule was obtained (see Fig. 5).

In Table 3, we have tabulated the BDE values that characterize the hydrogen atom donating ability in the gas phase. The BDE values have been compared to the phenol BDE (Wright et al., 2001). It is interesting to note that the hydrogen bonds influence on the stability of the radicals. The hydroxyl is the most important site for the H-atom transfer.

It can be seen that the BDE of SB4b–SB4d is smaller than phenol which revealed that abstraction of hydrogens at these
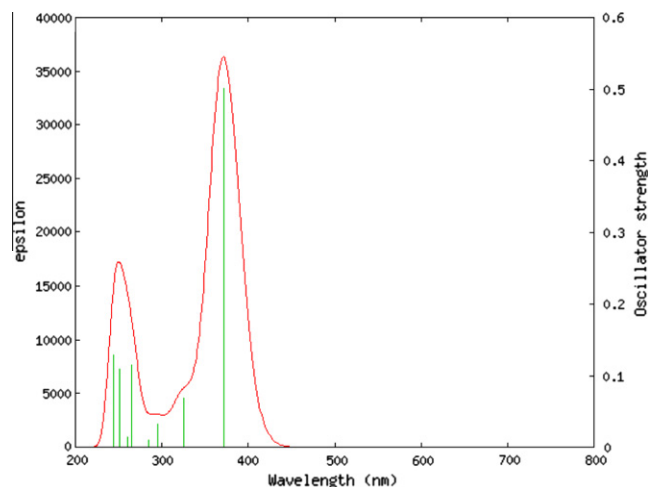

Figure 4 The absorption peaks of SB4 computed at TD-B3LYP/6-31G* level of theory.

positions would be favorable to enhance the antioxidant activity. The hydrogen abstraction at positions b and c would increase the activity having smallest BDE among all the investigated systems. The trend of antioxidant activity according to the positions has been observed as b > c > d > a ≅ phenol. From the BDE values presented in Table 3, it can be found that a smaller amount of energy is required for breaking the hydroxyl groups at positions b and c. The smaller BDE also revealed that hydrogen atom transfer reaction should first occur at b-OH and c-OH while hydrogen abstraction would not be favorable for a-OH and d-OH due to relatively higher BDE values. From Table 3, it can be seen that the BDE values of b-OH, c-OH and d-OH are smaller than the phenol which revealed that phenolic hydroxyls have a stronger aptitude toward donating the hydrogen atom/atoms. Furthermore, α-tocopherol is a biologically reference compound for antioxidant activity which is a lipid soluble chain-breaking antioxidant in human blood plasma having a BDE value of 72.3 kcal/mol (Burton and Ingold, 1986) which is smaller than the BDE of SB4b and SB4c, i.e., 67 and 68 kcal/mol, respectively.

4.6. Single electron transfer mechanism

The scavenging of free radicals by polyphenols may be achieved by donating single electron. The IP is an important physical factor revealing the range of electron transfer. According to the one-electron transfer, an electron is removed from the HOMO of the parent molecules, giving rise to radical cations. The investigated compounds have planar radical cations revealing there would be entire conjugation. The hydrogen bonds similar to the parent molecule are contributing to auxiliary stabilization. The IP value for SB4 is 155 kcal/mol which is 37 kcal/mol smaller than phenol illuminating electron transfer mechanism for the scavenging of free radicals. The electron transfer of SB4 would be similar to that of other flavonoids which have 30–40 kcal/mol smaller IP values than phenol (Ji et al., 2005). The low IP value compared to phenol revealed that SB4 would be a better antioxidant (see Table 3).

Table 2 Different descriptors of SB4 in eV obtained at B3LYP/6-31G* level of theory.

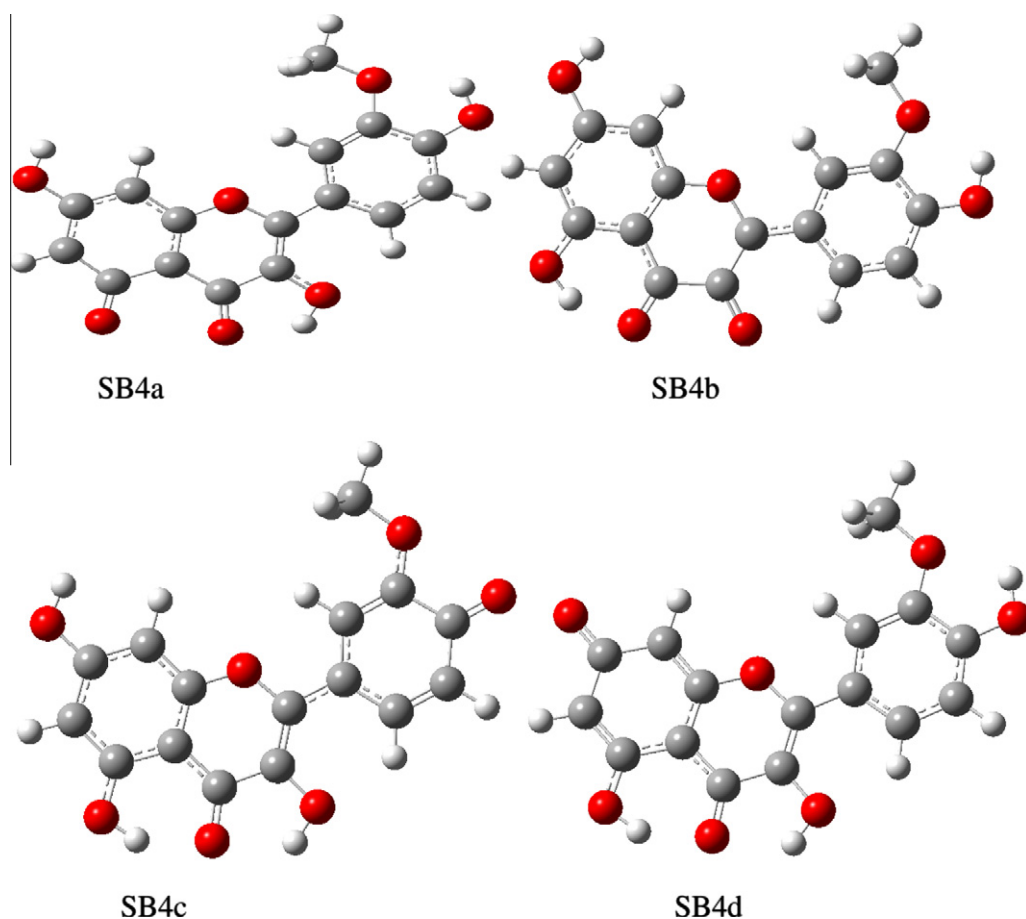| E$_{HOMO}$	E$_{LUMO}$	HOMO–LUMO gap	χ	η
−5.43	−1.82	3.61	3.63	1.81
ω	S	ωi	μ	
3.63	0.28	10.48	6.35	
HOMO-1–LUMO gap		HOMO-2–LUMO gap		
4.35		4.79		

Figure 5 The optimized structures of the radical cations investigated in the present study.

Table 3 The BDE and IP of SB4 in kcal/mol.

Compounds	BDE	IP	Compounds	BDE	IP
Phenol	83	192	–	–	–
SB4	–	155	SB4c	68	–
SB4a	83	—	SB4d	73	–
SB4b	67	–	–	–	–

5. Conclusions

The SB4abc is the most stable rotamer due to three H-bonding. The HOMO is delocalized on entire molecules and the lone pair of electron on the oxygen atoms. The LUMO is of antibonding character with π^* distributed on whole of the system. The two computed absorption peaks are prominent, i.e., at 371 nm which is absorption maxima and the second peak has been observed at 244 nm. The BDE of SB4b–SB4d is smaller than phenol which revealed that abstraction of hydrogens at these positions would be favorable to enhance the antioxidant activity. The hydrogen abstraction at positions b and c would increase the activity having smallest BDE among all the investigated systems. The IP value for SB4 is 155 kcal/mol which is 37 kcal/mol smaller than phenol illuminating electron transfer mechanism for the scavenging of free radicals.

References

Al-Sehemi, A.G., Al-Melfi, M.A.M., Irfan, A., 2012. Struct. Chem. http://dx.doi.org/10.1007/s11224-012-0103-2.

Al-Sehemi, A.G., Irfan, A., Aljubiri, S.M., Shaker, K.H., 2012. Arabian J. Chem. submitted.

Al-Yahya, M.A., Al-Meshal, I.A., Mosa, J.S., Al-Badr, A., Tariq, M., 1990. King Saud University Press, 64.

Antonczak, S., 2008. J. Mol. Struct. 856, 38–45, THEOCHEM.

Aron, P.M., Kennedy, J.A., 2008. Mol. Nutr. Food Res. 52, 79–104.

Belcastro, M., Marino, T., Russo, N., Toscano, M., 2006. Theor. Chem. Acc. 115, 361–369.

Burton, G.W., Ingold, K.U., 1986. Acc. Chem. Res. 19, 194–201.

Chattaraj, P.K., Lee, H., Parr, R.G., 1991. J. Am. Chem. Soc. 113, 1855–1856.

Cleland, D.M., Gordon, K.C., Officer, D.L., Wagner, P., Walsh, P.J., 2009. Spectrochim. Acta, Part A 74, 931–935.

El-Khatib, A.S., Khaleel, A.E., 1995. Bulletin of the Faculty of Pharmacy, Cairo University, 33(2): pp. 59–65.

El-Sayed, N.H., Mogahed, M.I., Haron, A.A., Mabry, T.J., 1998. Rev. Latinoam. Quim. 26 (3), 81–85.

Frisch, M.J. et al., 2009. Gaussian 09, Revision. Gaussian, Inc., Wallingford, CT.

Halliwell, B., 2007. Cardiovasc. Res. 73, 341–347.

Huang, M.-R., Li, S., Li, X.-G., 2010. J. Phys. Chem. B 114, 3534–3542.

Irfan, A., Al-Sehemi, A.G., 2011. J. Saudi Chem. Soc. http://dx.doi.org/10.1016/j.jscs.2011.11.006.

Ji, H.F., Tang, G.Y., Zhang, H.Y., 2005. QSAR Comb. Sci. 24, 826–830.

Kamel, M.S., Mohamed, K.M., Hassanean, H.A., Ohtani, K., Kasai, R., Yamasaki, K., 2001. Phytochemistry 57 (8), 1259–1262.

Kohn, W., Becke, A.D., Parr, R.G., 1996. J. Phys. Chem. 10, 12974–12980.

Leopoldini, M., Pitarch, I.P., Russo, N., Toscano, M., 2004a. J. Phys. Chem. A 108, 92–94.

Leopoldini, M., Marino, T., Russo, N., Toscano, M., 2004b. J. Phys. Chem. A 108, 4916–4922.

Manach, C., Mazur, A., Scalbert, A., 2005. Curr. Opin. Lipidol. 16, 77–84.

O' Boyle, N.M., Tenderholt, A.L., Langner, K.M., 2008. Cclib: a library for package-independent computational chemistry algorithms. J. Comp. Chem. 29, 839–845.

Parr, R.G., Pearson, R.G., 1983. J. Am. Chem. Soc. 105, 7512–7516.

Pietta, P.-G., 2000. J. Nat. Prod. 63, 1035.

Rizk, A.M., 1986. King Print of Richmond, 29.

Rosane, W.I., Oliveira, Z.D., Fernandes, S.C., Vieira, I.C., 2006. J. Pharm. Biomed. Anal. 41, 366–372.

Steiner, T., 2002. Angew. Chem. Int. Ed. 41, 48–76.

Steiner, T., Desiraju, G.R., 1998. Chem. Commun. 8, 891–892.

Walsh, P.J., Gordon, K.C., Officer, D.L., Campbell, W.M., 2006. J. Mol. Struct. Chem. 759, 17–24.

Wright, J.S., Johnson, E.R., DiLabio, G.A., 2001. J. Am. Chem. Soc. 123, 1173–1183.